

**DYNAMIC DEVICES - PICKUPS AND KICKERS\***

Glen Lambertson  
Lawrence Berkeley Laboratory  
University of California  
Berkeley, California 94720

**TABLE OF CONTENTS**

Introduction .....	1414
1. Relation Between Transverse and Longitudinal Effects .....	1415
2. Application of Reciprocity Theorem .....	1417
3. Response Functions .....	1418
4. Stripline Electrodes .....	1423
5. Capacitive Pickup .....	1427
6. Resonant Cavity .....	1430
7. Traveling-Wave Electrode .....	1433
8. Strong Magnetic Kicker .....	1435
9. Transverse Variation of Coupling .....	1439
References .....	1442

---

**\*This work was supported by the Director, Office of Energy Research, Office of High Energy and Nuclear Physics, High Energy Physics Division, U.S. Dept. of Energy, under Contract No. DE-AC03-76SF0098.**

## DYNAMIC DEVICES - PICKUPS AND KICKERS

Glen Lambertson  
Lawrence Berkeley Laboratory  
University of California  
Berkeley, California 94720

## INTRODUCTION

A large proportion of the dynamic devices used to interact with the charged-particle beams in accelerators or storage rings can be classified as pickups or kickers. These devices<sup>1</sup> act through time-varying electromagnetic fields either to extract information about the particle's motion or to effect a change in that motion. A given configuration of electrodes may be used either as a pickup or as a kicker; that duality will be addressed in this paper.

An example of a simple electrode is the loop antenna, which may be made in the shape of an electrical stripline at the side of a beam chamber. This electrode picks up a signal from the beam current by intercepting time-varying magnetic flux and image charges of the beam. One can also understand that the difference signal from two such striplines placed on opposite sides of the beam will give information on the beam's transverse position. This same electrode, if externally excited as a kicker, can produce transverse forces through its magnetic field acting on moving charges; and its electric fields in the direction of the particle motion produce its effects as a longitudinal kicker.

Electrodes for a particular application call for response over a particular range of frequencies. The stripline electrodes provide useful coupling over a range greater than one octave, centered about frequencies usually between 100 MHz and 10 GHz. In this same frequency region, a narrow-band device is the r.f. cavity which can be employed as either a sensitive pickup or a high-power accelerating or deflecting electrode; the rf accelerating system of a particle accelerator is a specialized example of such a kicker. A particular wave form with short rise time, then long flat dwell, is called for in the pulsed magnet kicker used to inject beam onto a closed orbit. Depending on the application, analysis, and description, an electrode's performance may be in either the time domain or the frequency domain.

In the discussion which follows, we shall derive some general relations between longitudinal and transverse effects, and between the responses as pickup and as kicker. We shall see that dynamic effects are entirely determined by the longitudinal electric fields in the direction of the beam current when the electrode is excited as a kicker; and as a corollary, absence of longitudinal electric fields

guarantees no coupling to beam particles. Response functions that serve as figures of merit will be defined. We shall then analyze the responses of specific examples of pickups and kickers. Finally, an approach to the calculation of the transverse variation of coupling over the electrode aperture will be presented.

### 1. RELATION BETWEEN TRANSVERSE AND LONGITUDINAL EFFECTS

The transverse deflection received by a moving particle is produced by field components that are transverse to the particle's velocity. However, in this section we shall show that in a time-varying electromagnetic field, the deflection can be expressed in terms of only the longitudinal component of electric fields in the kicker.

The total momentum deflection  $\Delta \vec{p}$  produced in a particle of charge  $e$  and velocity  $\vec{v}$  is

$$\Delta \vec{p} = e \int_a^b (\vec{E} + \vec{v} \times \vec{B}) dt \quad (1.1)$$

where  $\vec{E}$  and  $\vec{B}$  are the electric and magnetic fields the particle experiences in going from  $a$  to  $b$  along a trajectory  $d\vec{s} = \vec{v} dt$ . On that same path the particle will receive an energy change

$$\Delta E = e \int_a^b \vec{E} \cdot d\vec{s} \quad (1.2)$$

To the extent that we may treat the velocity  $\vec{v}$  as a constant vector, a simple relation may be found between derivatives of  $\Delta \vec{p}$  and  $\Delta E$ .

Examine

$$\frac{\partial}{\partial t} \Delta \vec{p} = e \int_a^b \left( \frac{\partial \vec{E}}{\partial t} dt + d\vec{s} \times \frac{\partial \vec{B}}{\partial t} \right) \quad (1.3)$$

in which we may insert

$$\frac{\partial \vec{B}}{\partial t} = - \nabla \times \vec{E} \quad (1.4)$$

and use the identity

$$\begin{aligned} \vec{ds} \times \vec{v} \times \vec{E} &= \vec{v} (\vec{ds} \cdot \vec{E}) - (\vec{ds} \cdot \vec{v}) \vec{E} \\ &= \vec{v} (\vec{ds} \cdot \vec{E}) - \frac{\partial \vec{E}}{\partial s} ds \end{aligned} \quad (1.5)$$

to obtain

$$\frac{\partial}{\partial t} \Delta \vec{p} = e \int_a^b \left[ -\vec{v} (\vec{ds} \cdot \vec{E}) + d\vec{E} \right] . \quad (1.6)$$

Separate this vector equation into components parallel to and transverse to trajectory  $s$ . The parallel component gives the identity

$$\frac{\partial}{\partial t} (\Delta p_s) = e \frac{\partial}{\partial t} \int_a^b E_s dt . \quad (1.7)$$

The result of interest is that, under the above assumption of a straight-line trajectory,

$$\begin{aligned} \frac{\partial}{\partial t} (\Delta \vec{p}_\perp) &= -e \int_a^b \left[ \vec{v}_\perp (\vec{E} \cdot \vec{ds}) - d\vec{E}_\perp \right] \\ \frac{\partial}{\partial t} \Delta \vec{p}_\perp &= -\vec{v}_\perp (\Delta E) + e \left[ \vec{E}_\perp(b) - \vec{E}_\perp(a) \right] . \end{aligned} \quad (1.8)$$

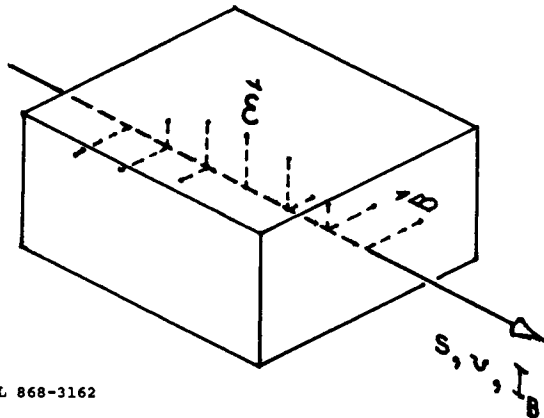
For many cases, the term containing entrance and exit fields is zero and the restriction to a straight-line trajectory is reasonable; therefore, this equation has many applications. For fields with sinusoidal variation  $e^{j\omega t}$ , the equation becomes

$$j\omega \Delta \vec{p}_\perp = -\frac{\partial}{\partial x} (\Delta E) . \quad (1.8a)$$

Several consequences of this relation come to mind:

- a. A sweeping transverse kicker will introduce an energy gradient across the beam width. But it is not necessary to have a static field to produce an acceleration that is uniform in space.
- b. The distribution of longitudinal electric fields  $E_{||}$  completely defines the transverse (and longitudinal) kick except for an additive static deflection.
- c. An rf cavity with no longitudinal  $E$  fields (i.e., pure TE modes) cannot produce a deflection.

This last conclusion is illustrated in Fig. 1 which shows the direction of fields encountered by a particle in passing through a resonating TE cavity. Eq. (1.8a) tells us that deflections from the  $E$  and the  $B$  fields must cancel exactly.



XBL 868-3162

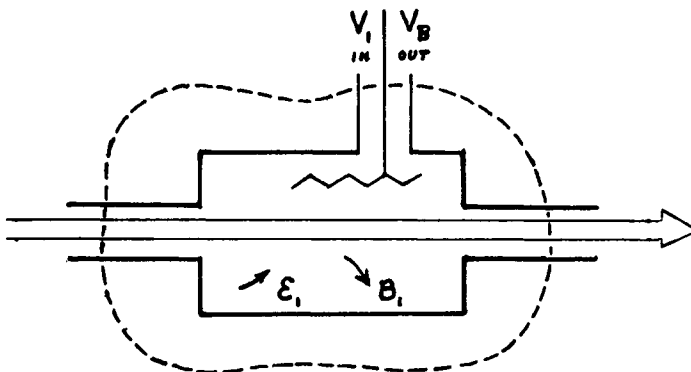
Fig. 1. TE-mode fields along beam trajectory through cavity.

## 2. APPLICATION OF RECIPROcity THEOREM

The Lorentz reciprocity theorem concerns a volume, bounded by surface  $S$ , that contains electromagnetic fields from two sources designated by subscripts 1 and 2. The sources may be current densities  $J$  within the volume or external sources that, in part, determine fields at the surface  $S$ . The basic form of the theorem, in which fields and currents are expressed as complex phasor vectors with time dependence  $e^{j\omega t}$ , is<sup>2</sup>

$$\oint_S (\vec{E}_1 \times \vec{H}_2 - \vec{E}_2 \times \vec{H}_1) \cdot d\vec{S} = \int_{\text{vol}} (\vec{E}_2 \cdot \vec{J}_1 - \vec{E}_1 \cdot \vec{J}_2) d \text{ vol} . \quad (2.1)$$

Apply this theorem<sup>3</sup> to the schematic diagram of a pickup in Fig. 2, where  $J_B$  is the beam current density and subscript B is used in place of 2. The outgoing signal produced at the signal port



XBL 868-3163

Fig. 2. Schematic pickup diagram for application of reciprocity theorem.

is  $V_B$ . The signal port may be a cable of characteristic impedance  $Z_C$ . Also at this port, an inwardly directed voltage  $V_1$  is supplied to produce within S field  $\vec{E}_1$  and  $B_1$  and currents  $J_1$  in resistive media; we shall ignore any perturbation produced in  $J_B$ . The volume integral over resistive media vanishes, leaving only the term in  $\vec{E}_1 \cdot J_B$  containing free current. The portion of the surface integral covering the entrance and exit beam ports may be made zero if the beam pipes are made small enough to prevent the propagation of traveling waves. At the signal port, entering and exiting TEM waves contribute two additive terms of  $V_1 V_B / Z_C$  to the surface integral. Therefore, Eq. (2.1) becomes

$$2 \frac{V_1 V_B}{Z_C} = - \int_{\text{vol}} \vec{E}_1 \cdot \vec{J}_B \, d \text{ vol}$$

or

$$V_B = - \frac{Z_C}{2V_1} \int_{\text{vol}} \vec{E}_1 \cdot \vec{J}_B \, d \text{ vol} \quad . \quad (2.2)$$

In this equation, note that  $J_B$  is a sinusoidal wave of beam current and the integral is evaluated at one instant in time. The usefulness of Eq. (2.2) stems from the observation that frequently it is simpler to calculate the fields in an electrode when excited by an external source  $V_1$  than to calculate directly the response when excited by a beam current. Later we shall also use this equation to find a relation between the responses of an electrode as a kicker and as a pickup.

### 3. RESPONSE FUNCTIONS

To describe the coupling between the terminals of an electrode and the beam, certain parameters are in common usage. These will be defined and then related using Eqs. (1.8) and (2.2). For this purpose, the frequency domain and complex vector notation will again be used.

For the longitudinal kicker, a convenient dimensionless parameter is the kicker constant  $K_{||}$ , which is simply the complex ratio of the change in beam particle energy (in volts) to the kicker input voltage  $V_K$ . The energy change is found by integrating the kicker fields  $\vec{E}_K$  along the particle path as in Eq. (1.2):

$$\frac{\Delta E}{e} = \int_S e^{j\omega t} \vec{E}_K \cdot d\vec{s} \quad . \quad (3.1)$$

The particle, having velocity  $\beta c$ , will be at position  $s$  when  $t = s/\beta c$ . Substitute this and  $k = \omega/\beta c$  to obtain the longitudinal kicker transfer function defined as

$$K_{\parallel} \equiv \frac{\Delta E}{eV_K} = \frac{1}{V_K} \int_S e^{jks} \vec{E}_K \cdot d\vec{s} . \quad (3.2)$$

As we have noted, the kicker constant  $K_{\parallel}$  is dimensionless and contains information on phase shift, but it is not uniquely related to the efficiency of an electrode because its magnitude may be changed by introducing a transformer at the terminals of the kicker to change the input impedance  $Z_c$ .

For a figure of merit more related to energy efficiency, we adopt the parameters used to describe an rf accelerating cavity, namely, shunt impedance, transit time factor, and cavity voltage. By analogy with cavity voltage, the instantaneous electrode voltage along the beam path is

$$V_o = \int_S \vec{E}_K \cdot d\vec{s} . \quad (3.3)$$

This differs from the voltage gain of a particle by the transit time factor defined as

$$T_{\parallel} = \Delta E / eV_o = V_K K_{\parallel} / V_o . \quad (3.4)$$

The shunt impedance  $R$  is defined in terms of the input power by the equation

$$P \equiv |V_o|^2 / 2R . \quad (3.5)$$

Noting that this kicker power is also given by  $|V_K|^2 / 2Z_c$ , we can use Eq. (3.4) to show that

$$RT^2 = Z_c |K_{\parallel}|^2 = \left| \frac{\Delta E}{e} \right|^2 / 2P . \quad (3.6)$$

The quantity  $RT^2$  may often be referred to as simply shunt impedance, but it is desirable to retain the  $T^2$  to indicate that it includes the transit time factor.  $R$  is directly related to the kicker electrode structure and  $T$  introduces the effect of the finite particle velocity.

For the transverse kicker, proceed in a similar manner starting with Eq. (1.1) to obtain

$$\vec{K}_{\perp} \equiv \frac{\Delta p_{\perp} \beta c}{eV_K} = \frac{1}{V_K} \int_S e^{jks} (\vec{E}_{\perp} + \vec{v} \times \vec{B})_K d\vec{s} \quad (3.7)$$

and

$$R_{\perp} T^2 = Z_c |K_{\perp}|^2 . \quad (3.8)$$

As was shown in section 1, the transverse and longitudinal kicks are related through the spatial gradient of  $\Delta E$ . Hence, using Eq. (1.8), we find that

$$-jk \vec{K}_\perp = \vec{V}_\perp K_\parallel \quad (3.9)$$

Turning our attention now to pickups, one of the more obvious choices for a coupling parameter is the ratio of pickup output voltage to beam current, which is defined as the longitudinal transfer impedance  $Z_p$ :

$$Z_p \equiv V_B / I_B \quad (3.10)$$

For a pickup intended to respond to the transverse position of the beam, the output signal is proportional to the product of current and displacement  $x$ ; such a pickup is characterized by a transverse transfer impedance

$$Z'_p \equiv \frac{1}{I_B} \frac{\partial V_B}{\partial x} = V'_B / I_B x \quad (3.11)$$

The reciprocity result Eq. (2.2) can now be used to relate  $Z_p$  to  $K$ . If we insert Eq. (2.2) in Eq. (3.10), we obtain

$$Z_p = - \frac{Z_c}{2V_1 I_B} \int_{\text{vol}} \vec{\epsilon}_1 \cdot \vec{J}_B \, d \text{vol} \quad (3.12)$$

(at fixed time)

In this volume integral, values of  $\epsilon$  and  $J$  are taken at a fixed time. The beam, assumed to be moving in the positive  $s$ -direction with velocity  $\beta c$ , will have an  $s$ -dependence  $e^{-jks}$ . Furthermore, assuming  $\vec{\epsilon}_1$  does not vary greatly over the beam cross section, we may integrate over  $x$  and  $y$  giving

$$\int_1 \vec{\epsilon}_1 \cdot \vec{J}_B \, dx dy = \vec{\epsilon}_1 \cdot \vec{I}_B e^{-jks} \quad (3.13)$$

and  $Z_p$  becomes

$$Z_p = - \frac{Z_c}{2V_1} \int_s e^{-jks} \vec{\epsilon}_1 \cdot \vec{ds} \quad (3.14)$$

This integral differs from that in Eq. (3.2) defining  $K_\perp$  only in the sense of  $s$ . Therefore, it represents a kicker excited with  $V_1$ , but with the beam waves traveling in the reversed direction. The relation between pickup and kicker responses for a given electrode is therefore

$$Z_P = \frac{1}{2} Z_c K_{\parallel} \quad (3.15)$$

with the provision that the beam sense be reversed between the two applications. This technicality concerning the sense of the beam's motion takes into account the very real directional sensitivity of some beam electrode structures.

The similar relation for transverse responses is obtained by differentiating Eq. (3.15) with respect to  $x$ ,

$$Z_P' = \frac{1}{2} Z_c \frac{\partial K_{\parallel}}{\partial x} \quad (3.16)$$

and using Eq. (3.9), giving

$$Z_P' = -\frac{1}{2} j k Z_c K_{\perp} \quad (3.17)$$

The power from the pickup signal into an impedance-matched load,  $Z_c$ , is

$$P_P = \frac{1}{2} (I_B Z_P)^2 / Z_c \quad (3.18)$$

We may rewrite this in terms of the electrode's (kicker) shunt impedance using Eq. (3.15) and Eq. (3.6) to obtain, for the longitudinal pickup,

$$P_P = \frac{1}{2} I_B^2 Z_c \left(\frac{1}{2} K_{\parallel}\right)^2$$

$$P_P = \frac{1}{2} I_B^2 (R_{\parallel} T^2 / 4) \quad (3.19)$$

Here we see that the shunt impedance (modified by the factor 1/4) serves also as a measure of efficiency of that electrode used as a pickup. Similarly, for the transverse pickup, we obtain the power

$$P_P' = \frac{1}{2} (I_B x Z_P')^2 / Z_c$$

or

$$P_P' = \frac{1}{2} (I_B x)^2 k^2 (R_{\perp} T^2 / 4) \quad (3.20)$$

The appearance of  $k = \omega/\beta c = 1/\beta\lambda$  in the transverse electrode responses has the consequence that a pickup configuration, if used as a kicker, will have a comparatively lower response at high frequency. With this qualification, we see that high shunt impedance relates to high efficiency for an electrode whether used as a pickup or a kicker.

Application of the reciprocity-derived relations assumes that voltage  $V_k$  and  $V_p$  are observed at an impedance-matched connection where no reflected waves are present. This is not always the case at convenient electrode terminals and mismatch introduces some modification in the relations so far derived.

A resonant electrode without driver or amplifier input impedance connected is characterized by an unloaded Q-value,  $Q_U$ . With driver or load attached, the total circuit response is widened to  $\Delta\omega/\omega = Q_L$  which depends on the load and how it is coupled to the electrode. (In some applications the degree of loading may conveniently be used to adjust the response width.) At the terminals of a kicker, of course, the driver impedance has no effect on  $K$  or  $RT^2$ , but the efficiency of the driver is affected by any impedance mismatch. On the other hand, at the terminals of a pickup the output voltage ( $Z_p$ ) and power at the unmatched load do depend on the loading. Maximum power is delivered when a matched load lowers  $Q_L$  to one-half  $Q_U$ . For other degrees of loading, the value of  $Z_p$  at resonance is multiplied by  $2Q_L/Q_U$  and the power by the factor  $4Q_L(Q_U - Q_L)/Q_U^2$ .

Table I is a summary of useful relations for beam electrodes. These apply at any frequency other than zero. The special considerations for unmatched loading of resonant systems are not incorporated here.

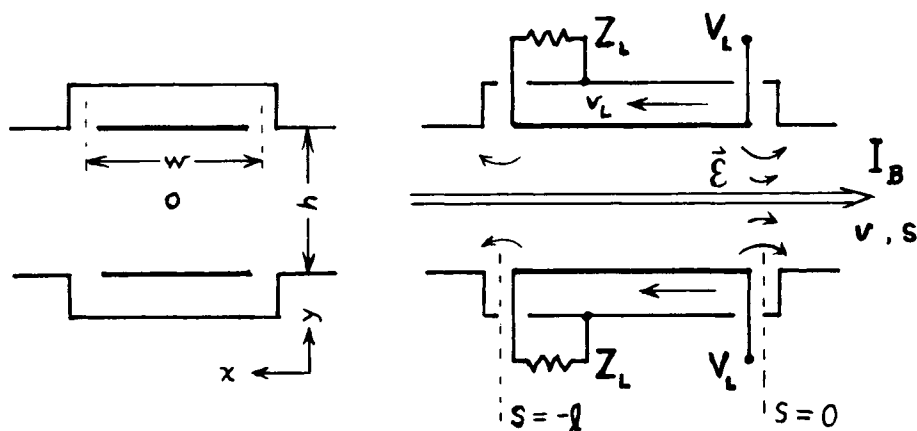
Table I

	Longitudinal	Transverse
kicker	$\frac{\Delta E}{e} = K_{\parallel} V_K$	$\frac{\Delta p_{\perp} \beta c}{e} = K_{\perp} V_K$
	$\vec{V}_{\perp} K_{\parallel} = -jk \vec{K}_{\perp}$	
	$P_K = \frac{1}{2} \left  \frac{\Delta E}{e} \right ^2 / R_{\parallel} T^2$	$P_K = \frac{1}{2} \left  \frac{\Delta p_{\perp} \beta c}{e} \right ^2 / R_{\perp} T^2$
	$R_{\parallel} T^2 = Z_c  K_{\parallel} ^2$	$R_{\perp} T^2 = Z_c  K_{\perp} ^2$
	$Z_p = \frac{1}{2} Z_c K_{\parallel}$	$Z_p' = -\frac{1}{2} jk Z_c K_{\perp}$
pickup	$V_p = Z_p I_B$	$V_p' = Z_p' (I_B \times)$
	$P_p = \frac{1}{2} I_B^2 (R_{\parallel} T^2 / 4)$	$P_p' = \frac{1}{2} (I_B \times)^2 k^2 (R_{\perp} T^2 / 4)$

## 4. STRIPLINE ELECTRODES

In this section we shall calculate in some detail the responses of stripline electrodes to illustrate the application of the relations in Table I. To do this we must first visualize the electromagnetic waves in a structure such as the stripline pair diagrammed in Fig. 3.

Each of the stripline plates with its adjacent ground plane (walls) forms a transmission line for TEM waves. In the center (away from the ends) of these short lines the fields are purely transverse and propagating at a line velocity  $V_L$ . That velocity would be the velocity of light for smooth two-dimensional conductors, but may be reduced by the presence of magnetic or dielectric media or by longitudinal variations in the cross sections of the conductors. Each stripline has a characteristic impedance  $Z_L$ , the value of which is modified somewhat by coupling to the other line. At the ends of the strips, longitudinal electric fields arise. It is the integral, Eq. (3.1), through these fields that determines the coupling of the beam electrode as a kicker, and using the mathematical relations of Table I, also the coupling as a pickup with beam velocity reversed. While this formalism will give the response of the pickup, it may be more satisfying to visualize the distributions of induced currents as the physical mechanism for coupling by the pickup.



XBL 868-3164

Fig. 3. A pair of stripline electrodes.

The configuration shown in Fig. 3 makes a simple broad-band electrode. The sense of the beam velocity and the polarities of the exciting voltages shown are appropriate for its use as a longitudinal kicker powered by signals at the downstream end. In each strip-line a wave propagates upstream and is terminated in its line impedance  $Z_L$ . The voltage to drive the kicker,  $V_K e^{j\omega t}$ , will usually be supplied at  $R_0 = 50$  ohms impedance and must be transformed to  $Z_L$  and divided to provide voltage  $V_L$  for each line. The voltage needed is thus  $V_K = V_L \sqrt{2R_0/Z_L}$ .

We want to calculate the kicker function using Eq. (3.2)

$$K_{\parallel} = \frac{\Delta E}{eV_K} = \frac{1}{V_L} \sqrt{\frac{Z_L}{2R_0}} \int_{s=vt} e^{j\omega t} \vec{\epsilon}_K \cdot d\vec{s} \quad (4.1)$$

which involves only the longitudinal components of field  $\epsilon_K e^{j\omega t}$  evaluated at the position of the beam particle, i.e., at  $s = vt$ . The fields are concentrated at the ends  $s = -l$  and  $s = 0$ . The integral through one end field is less than the line voltage by a geometric factor  $g_{\parallel}(w, h)$  which reflects the fraction of the angular space around the beam subtended by the electrodes and it is also reduced by a transit-time factor which we shall assume is near unity for a short gap and high velocity particle. (These factors will be discussed more in Section 9.) For a beam on the centerline of this configuration, the geometric factor may be shown to be

$$g_{\parallel} = \frac{2}{\pi} \tan^{-1} \left( \sinh \frac{\pi w}{2h} \right), \quad (4.2)$$

an expression whose value exceeds 0.95 for  $w/2h > 1$ . Therefore, for the s-component in Eq. (4.1), we take

$$\epsilon_s e^{j\omega t} = g_{\parallel} V_L \left[ \delta(s) - \delta(s+l) \right] e^{j\omega(t + s/v_L)} \quad (4.3)$$

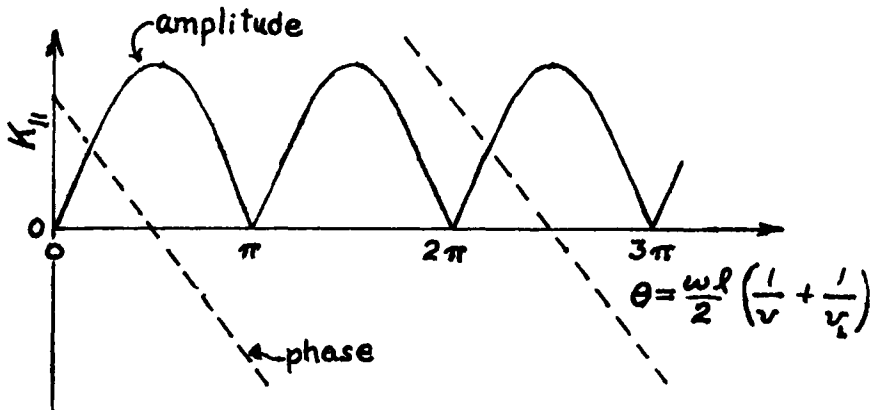
and insert for  $t$  the particle arrival time  $t = s/v$  to obtain

$$K_{\parallel} = \frac{1}{V_L} \sqrt{\frac{Z_L}{2R_0}} \int_{< -l}^{> 0} g_{\parallel} V_L \left[ \delta(s) - \delta(s+l) \right] e^{j\left(\frac{1}{v} + \frac{1}{v_L}\right)\omega s} ds$$

giving the kicker function

$$K_{\parallel} = \sqrt{\frac{Z_L}{2R_0}} 2g_{\parallel} e^{j\left(\frac{\pi}{2} - \theta\right)} \sin \theta \quad (4.4)$$

with  $\theta = \left(\frac{1}{v} + \frac{1}{v_L}\right) \frac{\omega l}{2}$ . This is shown in Fig. 4, which may be regarded as the response to either frequency, length, or velocity. If both beam and line velocities equal  $c$ , then  $K_{\parallel}$  is maximum and real for  $l = \lambda/4$ ; for this reason, the electrode is often called the



XBL 868-3165

Fig. 4. The longitudinal kicker function for striplines.

"quarter-wave loop". Note that at this maximum a passing particle receives a voltage kick  $2V_L g_{\parallel}$ , about twice the line voltage. It is a broad-band device that provides a bandwidth of an octave width at 1.25 dB down or a 3-to-1 range at 3 dB down.

Power for broad-band, high frequency operation is expensive, motivating one to maximize the shunt impedance which is, using Eq. (3.6),

$$R_{\parallel}^2 = 2Z_L g_{\parallel}^2 \sin^2 \theta. \quad (4.5)$$

Note that, as mentioned before, in this more fundamental figure of merit the source (or terminal) impedance  $R_0$  does not appear. At frequencies below about 100 MHz, the use of ferrite is very effective for increasing  $Z_L$  and shortening the electrode length. At very high frequencies, a lower ratio  $w/h$  may reduce  $g_{\parallel}$ ; also, waveguide modes may propagate in the gap  $h$  and modify the response.

When the stripline is used as a pickup, the beam must pass in the opposite sense so that the output terminals are upstream. Using  $Z_p = \frac{1}{2} R_0 K_{\parallel}$ , then we find the transfer impedance,

$$Z_p = \sqrt{\frac{R_0 Z_L}{2}} g_{\parallel} e^{j(\frac{\pi}{2} - \theta)} \sin \theta. \quad (4.6)$$

Typical stripline electrodes<sup>4,5</sup> have single-line impedance in the range 25-to-100 ohms and  $g^2 \approx \frac{1}{2}$ , giving at maximum response

$$\begin{aligned} R_{||} T^2 &\approx 25 - 100 \Omega \\ Z_p &\approx 18 - 35 \Omega \\ K_{||} &\approx 0.7 - 1.4 . \end{aligned}$$

A recent application of stripline electrodes in which weak signal and costly power were concerns was in the Fermilab antiproton accumulator.<sup>6</sup> Electrodes having a response range of 1-to-2 GHz and  $Z_L \approx 100$  ohms were used in 128-element arrays giving  $R_{||} T^2 = (128)$  (130) = 16.6 k $\Omega$  and  $Z_p = 40 \sqrt{128} = 450 \Omega$ .

Examination of striplines used as transverse electrodes illustrates some additional points. We shall calculate the response first using longitudinal fields only, as above, then by the intuitively more direct approach of integrating the transverse forces.

We use the same configuration as in Fig. 3, but reverse the polarity of the upper stripline making the  $\mathcal{E}_s$  fields be zero at center ( $y=0$ ) and vary approximately linearly as  $2y/h$ . The change in polarity will also change the factor  $g$ ; call this transverse geometric factor  $g_{\perp}$ , which at centerline is

$$g_{\perp} = \tanh \frac{\pi w}{2h} . \tag{4.7}$$

The coupling between the two striplines also changes producing a lower value for  $Z_L$ . The longitudinal kicker function  $K'_{||}$  for this so-modified case is thus, using Eq. (4.4),

$$K'_{||} = \frac{2Y}{h} \sqrt{\frac{Z_L}{2R_0}} 2g_{\perp} e^{j(\frac{\pi}{2} - \theta)} \sin \theta . \tag{4.8}$$

Apply Eq. (3.9) to find  $K_{\perp}$ :

$$\begin{aligned} K_{\perp} &= \frac{j}{k} \frac{\partial K'_{||}}{\partial y} \\ K_{\perp} &= \sqrt{\frac{Z_L}{2R_0}} 4g_{\perp} \frac{v}{hw} e^{-j\theta} \sin \theta . \end{aligned} \tag{4.9}$$

This result is very similar to the longitudinal  $K$  in Eq. (4.4), but the factor  $1/hw$  further penalizes large aperture and shifts the frequency for maximum response downward to  $\omega = 0$ . This will be more recognizable as a typical  $\sin\theta/\theta$  transit-time response if we rearrange using  $\theta = (\frac{1}{v} + \frac{1}{v_L}) \frac{\omega l}{2}$  :

$$K_{\perp} = \sqrt{\frac{Z_L}{2R_0}} 2g_{\perp} \frac{l}{h} \left(1 + \frac{v}{v_L}\right) e^{-j\theta} \frac{\sin \theta}{\theta} . \quad (4.9a)$$

The other characterizing parameters for the transverse case are obtained from Eq. (3.8) and (3.17):

$$R_{\perp} T^2 = 2Z_L \left(g_{\perp} \frac{2v}{h\omega}\right)^2 \sin^2 \theta \quad (4.10)$$

$$Z'_{\perp} = \sqrt{\frac{R_0 Z_L}{2}} g_{\perp} \frac{2}{h} e^{j(\frac{\pi}{2}-\theta)} \sin \theta . \quad (4.11)$$

This transverse transfer function does not contain the  $1/\omega$  factor and, except for the small difference between  $g_{\parallel}$  and  $g_{\perp}$  (and numerically different  $Z_{\perp}$ ) is the same as the longitudinal case divided by the half-gap.

The alternative approach using transverse fields starts from Eq. (3.7), using as the fields of the upstream TEM wave between the striplines:

$$\epsilon_y e^{j\omega t} = g_{\perp} v_L \frac{2}{h} e^{j\omega(t + \frac{s}{v_L})} \quad (4.12)$$

$$B_x e^{j\omega t} = \frac{1}{v_L} \epsilon_y e^{j\omega t} \quad (4.13)$$

to get

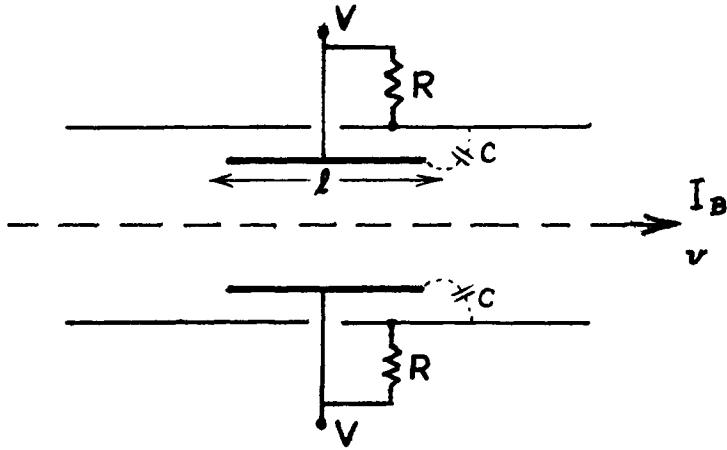
$$K_{\perp} = \frac{1}{v_L} \sqrt{\frac{Z_L}{2R_0}} \int_{-l}^0 e^{\frac{j\omega s}{v_L}} g_{\perp} v_L \frac{2}{h} e^{\frac{j\omega}{v_L} s} ds \quad (4.14)$$

which gives the same result as Eq. (4.9) and (4.9a). This latter approach in this case is simpler, but the object here has been to show the equivalence of the two.

A curious feature of the stripline pickup is that, if the beam velocity  $v$  equals the line velocity  $v_L$ , no voltage appears at the downstream end. This allows that end to be electrically connected to any impedance, including a short or an open circuit, with no effect on the picked-up signal. However, the output line will then not be back-terminated to absorb reflections in the circuit.

## 5. CAPACITIVE PICKUP

A plate or button that is exposed to the electric field of a beam will, in developing an image charge, drive current into a grounding resistor  $R$  (Fig. 5).



XBL 868-3166

Fig. 5. Schematic diagram of capacitive pickup.

A pair of electrodes connected in parallel will have a total image charge of

$$q = - g l I_B / v \tag{5.1}$$

where the effective length  $l$  and the geometric factor  $g$  are determined by the electrode size and distance from the beam  $I_B$  of positive particles. If the electrode pair completely encircled the beam, the factor  $g$  would be near unity.

First consider electrodes short compared to  $\lambda = 1/k$ , each of the two having capacitance  $C$  to ground. The voltage developed across the two resistors in parallel is

$$V = - j\omega q \frac{R/2}{1 + j\omega RC} = I_B j \frac{g\omega l}{2v} \frac{R}{1 + j\omega RC} \tag{5.2}$$

If, perhaps at low frequency,  $R$  is the direct input impedance of an amplifier, then  $V$  is the available signal, but usually undesired added capacitance to a remote connection or a transformer to  $R_o = 50 \Omega$  will result in only a fraction  $\alpha$  of the power being delivered to  $R_o$ . In that case we find

$$Z_p = \sqrt{\frac{2\alpha R_o}{R}} \frac{V}{I_B} = \frac{1}{2} \frac{jg\omega l}{2v} \frac{\sqrt{2\alpha R_o R}}{1 + j\omega RC} \tag{5.3}$$

Although with this unmatched load the equations of Table I are not strictly applicable, we can use them to find an effective  $RT^2$  for this pickup case:

$$RT^2 = 2 \left( g \frac{\omega l}{v} \right)^2 \frac{\alpha R}{1 + (\omega RC)^2} \quad (5.4)$$

At low frequencies, the signal is proportional to the rate of change of beam current, but above  $\omega RC \approx 1$ , the capacitance is said to "integrate" the signal and the resulting response is

$$Z_p \rightarrow \sqrt{2\alpha \frac{R}{R^2} g l / 2v C} \quad (5.5)$$

This region of flat response, although not the most sensitive because it calls for  $RC > 1/\omega$ , is often used for the observation of beam current versus time with a wide frequency range.

A stronger response over a more narrow band is provided if an inductor is placed in parallel with each R of Fig. 5. The resulting resonant circuits have a loaded  $Q_L = \omega_r RC$ , where R includes circuit losses and the output load. The picked-up capacitive currents then drive the parallel impedances  $Q_L / \omega_r C$  to produce at resonant frequency  $\omega_r$  the maximum pickup response

$$Z_p = j g \frac{\omega l}{2v} \sqrt{\frac{2\alpha R Q_L}{\omega_r C}} \quad (5.6)$$

and

$$RT^2 = 2 \left( g \frac{\omega_r l}{v} \right)^2 \frac{\alpha Q_L}{\omega_r C} \quad (5.7)$$

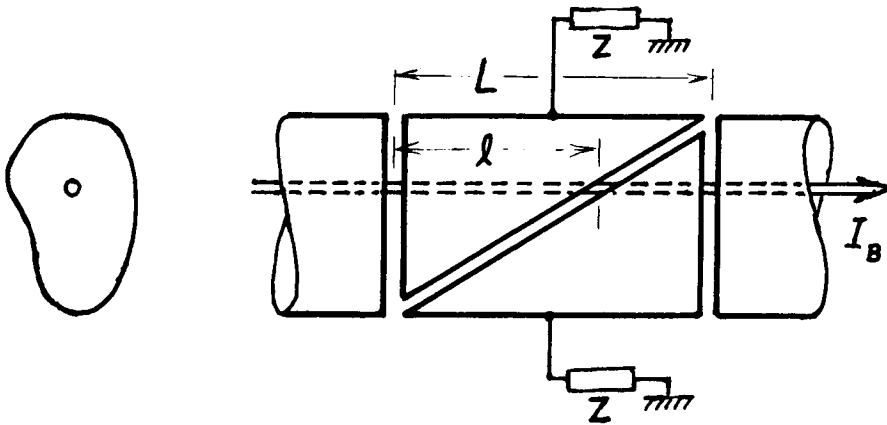
These quantities give the dependence of the resonant maximum on  $\omega_r$  and loaded Q. The band width is then  $\Delta\omega = \omega_r / Q_L$  at 3 dB reduction. The upper limit on Q is determined by losses in circuit components; in the neighborhood of 10 MHz where ferrite is still effective, a Q of  $\sim 100$  is available.

Resonating the capacitive pickup provides a controllable response width in a compact electrode at low frequencies where the wavelength would make a quarter-wave stripline or a cavity prohibitively large. In the intermediate length where, to maximize signal, the capacitive electrode length becomes comparable with  $\lambda$ , it may be analyzed as a center-connected open-ended strip transmission line. In that case, a characteristic line impedance of  $Z_L$  and velocity  $v_L$  are assumed and one can show that

$$RT^2 = 4 Z_L g^2 \frac{\sin^2 k l / 2}{\cos k_L \frac{l}{2} \sin k_L \frac{l}{2}} \alpha Q_L \quad (5.8)$$

where  $k_L = \omega_r/v_L$ . This becomes the same as Eq. (5.7) for small  $k_L \ell$ , using the relation  $Z_L v_L C = \ell$  for a TEM line. The cosine factor in the denominator approaches zero for a half-wave line, suggesting very high shunt impedance. Unfortunately, difficulties in coupling to a very low circuit impedance and other resonances enter to limit the open-ended electrode to less than a half wavelength long.

An electrode with transverse response linear with beam displacement (or uniform in deflection if used as a kicker) is formed by separating halves of a section of beam tube by a diagonal cut (Fig. 6). It is reasonable that linearity will result for some geometry, but that this is true for any shape cylindrical tube with diagonal cut is discussed in section 9.



XBL 868-3167

Fig. 6. Diagonally cut cylinder electrode.

6. RESONANT CAVITY

The cavity resonator is a very efficient beam coupler with, for simple shapes, predictable response within its resonant bandwidth. It is well suited for detecting or controlling by feedback particular modes of beam instability. Pickup or kicker circuitry is coupled to the cavity through a loop or stub antenna. That loading resulting from such coupling broadens the frequency response as noted in section 3; however, for characterizing the efficiency of a cavity, the unloaded shunt impedance  $RT^2$  at resonance is used. In this section we shall show how to calculate that impedance for both longitudinal and transverse kickers.

As an example of a sum pickup or kicker, consider the square cavity of Fig. 7. The shunt impedance is found from

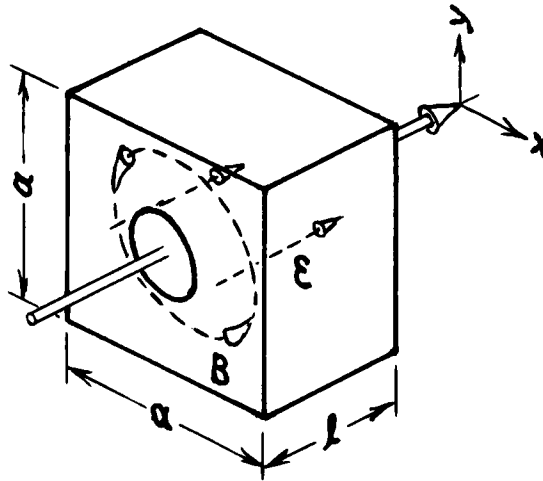
$$P = \frac{\omega_r U}{Q_U} = \frac{1}{2} \frac{\Delta E}{e}^2 / R_{\parallel} T^2 \quad (6.1)$$

using

$$\frac{\Delta E}{e} = \int e^{jkz} \epsilon_z dz \quad (6.2)$$

and

$$U = \frac{1}{2} \epsilon_0 \int_{\text{vol}} \epsilon^2 d \text{ vol} \quad (6.3)$$



XBL 868-3168

Fig. 7. Fields in longitudinal cavity-electrode.

The lowest cavity mode with maximum longitudinal electric field along the centerline is mode  $TM_{110}$  for which the wavelength is  $\lambda = \sqrt{2} a$  and the electric field is

$$\epsilon = \epsilon_0 \cos \frac{\pi x}{a} \cos \frac{\pi y}{a} \quad (6.4)$$

uniform in the z-direction. Application of Eq. (6.2) at  $x = y = 0$  gives

$$\frac{\Delta E}{e} = \epsilon_0 l \frac{\sin \theta}{\theta} \equiv \epsilon_0 l T \quad (6.5)$$

with  $\theta = \omega_r l / 2v = k_0 l / 2\beta$ . From Eq. (6.3) we find

$$U = \frac{1}{8} \epsilon_0 \epsilon_0^2 l a^2 \quad (6.6)$$

Substitute in Eq. (6.1) to obtain

$$R_{\parallel} T^2 = \frac{4}{\pi} \mu_0 c \frac{l}{\lambda} Q T^2 = 480 \frac{l}{\lambda} Q T^2 \text{ ohm} \quad (6.7)$$

As an example of another shape, for a circular cavity (pillbox), one can find that

$$R_{\parallel} T^2 = \frac{2}{\left[ \rho_{01} J_1(\rho_{01}) \right]^2} \mu_0 c \frac{l}{\lambda} Q T^2 \quad (6.8)$$

in which  $\rho_{01} = 2.405$ , giving

$$R_{\parallel} T^2 = 484 \frac{l}{\lambda} Q T^2 . \quad (6.8a)$$

A broad maximum value of the quantity  $lQT^2/\lambda$  occurs for  $\beta=1$  at  $\theta = 1.37$  radian at which  $l/\lambda = 0.37$  and  $T^2 = 0.51$ . At that optimum length, the simple cavity then gives

$$R_{\parallel} T^2 \approx 108 Q \text{ ohm} . \quad (6.9)$$

By modifying the cavity shape (e.g., reducing the longitudinal gap in the region immediately surrounding the beam tube), this figure may be increased about 25%.

In these equations, the unloaded quality factor,  $Q_U$  is used. This may be in the region of 30,000 at 1 GHz, for example, and varies as  $\sqrt{l/\omega}$ . When coupled to an external circuit, the bandwidth is controlled by the loaded  $Q_L$  and then, to calculate the power into an external load when used as a pickup, one must correct for any mismatch of impedance by changing  $RT^2$  used in Eq. (3.19) according to

$$RT^2 \rightarrow [4 Q_L(Q_U - Q_L)/Q_U^2] RT^2 . \quad (6.10)$$

A cavity in which the magnetic field transverse to the beam is as shown in Fig. 8 can serve as a transverse electrode. For a cavity with square cross section excited in the  $TM_{120}$  mode, the  $\epsilon_z$  field is

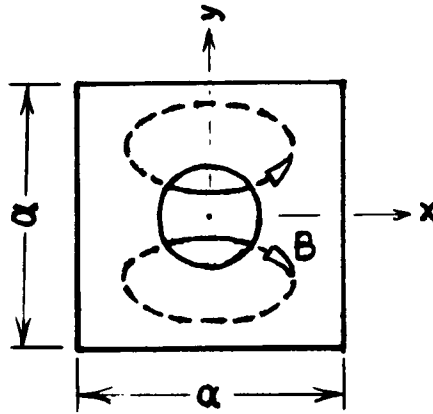
$$\epsilon = \epsilon_0 \cos \frac{\pi x}{a} \sin \frac{2\pi y}{a} \quad (6.11)$$

and  $\lambda = 2a/\sqrt{5}$ . We find  $R_{\perp} T^2$  using

$$P = \frac{\omega U}{Q} = \frac{1}{2} \left| \frac{\Delta p \beta c}{e} \right|^2 / R_{\perp} T^2 \quad (6.12)$$

in which

$$\frac{\Delta p \beta c}{e} = j \frac{\beta}{k_0} \frac{\partial}{\partial x} \left( \frac{\Delta E}{e} \right) = j \frac{\beta}{k_0} \frac{2\pi}{a} \epsilon_0 l T . \quad (6.13)$$



XBL 868-3169

Fig. 8. Field in transverse cavity-electrode.

T and U are the same as in Eqs. (6.5) and (6.6), giving the result

$$R_{\perp} T^2 = \frac{32}{25\pi} \mu_0 c \beta^2 \frac{\ell}{\lambda} Q T^2 = 153.6 \beta^2 \frac{\ell}{\lambda} Q T^2 \quad (6.14)$$

At maximum  $\ell Q T^2 / \lambda$  (and  $\beta=1$ ), we have  $\theta = 1.41$  and  $R_{\perp} T^2 = 33.7 Q$  ohm.

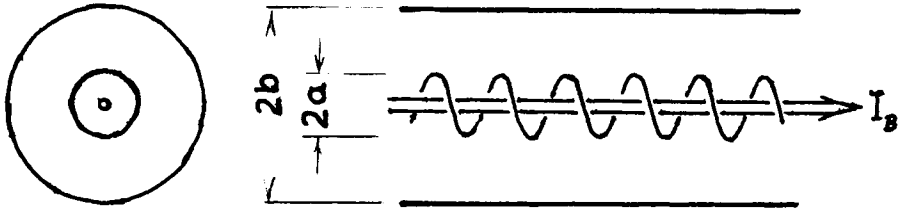
## 7. TRAVELING-WAVE ELECTRODE

Because coupling to the energy of the beam is through the longitudinal electric field, it is appealing to think of an electrode in which the wave of  $E_z$  moves downstream in velocity synchronism with the beam. To the extent that is achievable, the power interchanged will increase as  $\ell^2$ , instead of  $\ell$ . In smooth conducting waveguides the phase velocity is always greater than  $c$ , especially in modes with strong axial electric field. But some modified, or loaded, guides have slow waves and can be used as beam electrodes.<sup>7</sup>

On the axis of a helical line (Fig. 9), there is a longitudinal electric field with reduced velocity  $\beta_L c$ .<sup>8,9</sup> The shunt impedance of this electrode treated as a sheath helix is given by

$$R_{\parallel} T^2 = \left( \frac{h}{\gamma_L} \right)^2 \frac{\mu_0 c}{2\pi\beta_L} \left[ \frac{K_0(ha)}{I_0(ha)} - \frac{K_0(hb)}{I_0(hb)} \right] \left( \frac{\sin \theta}{\theta} \right)^2 \quad (7.1)$$

in which  $\gamma_L^2 = \frac{1}{1 - \beta_L^2}$ ,  $h = \frac{k_0}{\beta_L \gamma_L}$ , and  $\theta = \left( \frac{1}{\beta_B} - \frac{1}{\beta_L} \right) \frac{k_0 \ell}{2}$ . The



XBL 868-3170

Fig. 9. Beam on axis of helical line.

modified Bessel functions  $I_0$  and  $K_0$  for small arguments, that is, for  $\beta_L \gamma_L r \gg b$ , reduce to the form

$$R_{||} T^2 \approx \left( \frac{\omega l}{\beta_L \gamma_L^2 c} \right)^2 \frac{\mu_0 c}{2\pi \beta_L} \ln \frac{b}{a} \left( \frac{\sin \theta}{\theta} \right)^2 . \tag{7.1a}$$

In this we recognize  $(\mu_0 c / 2\pi) \ln(b/a)$  as the impedance of a coaxial line of radii  $a$  and  $b$ . Also, we see  $\sin \theta / \theta$  as the transit-time factor in which  $\theta$  is a measure of the phase slip between beam and traveling wave. To avoid large dispersion in the wave velocity in this periodic structure,  $\beta_L \lambda$  must be larger than twice the pitch of the helix. In an example use,<sup>10</sup> this electrode was effective at  $f = 200$  MHz,  $\beta = 0.5$ . However, the factor  $\gamma_L^4$  in the denominator will make the device ineffective for very relativistic particles.

The slotted-coax coupler shown in Fig. 10 communicates with the beam tube through a row of holes or slots in the outer wall of a coaxial line parallel to the beam.<sup>11</sup> There is a net energy transfer from a beam particle to the coaxial line until either an equilibrium is reached or a sufficient phase difference develops between beam and coax signal. The slots that provide the coupling also reduce the phase velocity in the coax and cause dispersion in that velocity. Perturbation calculations<sup>12</sup> for the geometry of Fig. 10 show that the coupling and the velocity are so related that the pickup impedance becomes simply

$$Z_p \approx -j \frac{\omega l}{2\gamma_L^2 c} \frac{r}{b} \sqrt{Z_L R_0} e^{-j\theta} \frac{\sin \theta}{\theta} \tag{7.2}$$

where  $Z_L$  is the impedance of the coax and  $\gamma_L$  and  $\theta$  are as in Eq. (7.1). The shunt impedance is then

$$R_{||} T^2 \approx \left( \frac{\omega l}{\gamma_L^2 c} \frac{r}{b} \right)^2 Z_L \left( \frac{\sin \theta}{\theta} \right)^2 . \tag{7.3}$$

This is very similar to the result for the helix, but here a very small velocity reduction introduces dispersion that limits the use of the slotted coupler as a broad-band device to  $\beta_1 > \sim 0.95$ . Although it is a weak coupler, it is a good high-frequency structure and is useful where strong coupling is not demanded.

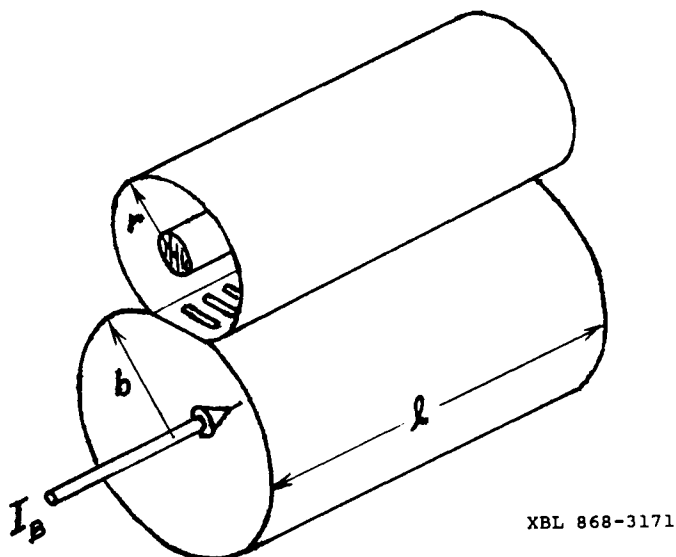
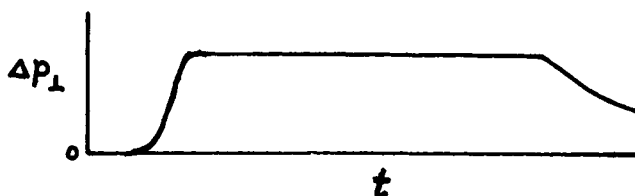


Fig. 10. Slotted coax on beam tube.

#### 8. STRONG MAGNETIC KICKER

A pulsed magnet with a field held steady during the passage of a burst of particles is usually the choice for injecting or ejecting beam from the orbit in a circular accelerator. The field in this device is commonly required to rise (or fall) rapidly during the gap between successive beam bunches or injection bursts (Fig. 11).



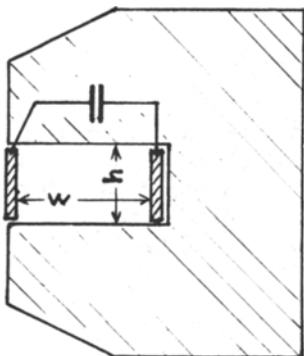
XBL 868-3172

Fig. 11. Pulse shape for ejecting circulating beam.

The overall length of such a device may be limited by space available as well as other considerations. Hence the beam gap  $v\tau$ , overall length  $l$ , and, of course, the deflection  $\Delta p$ , are primary design requirements. Minimum width and height,  $w$  and  $h$ , of the aperture are also predetermined. The values of most other parameters of the kicker are then narrowly constrained.

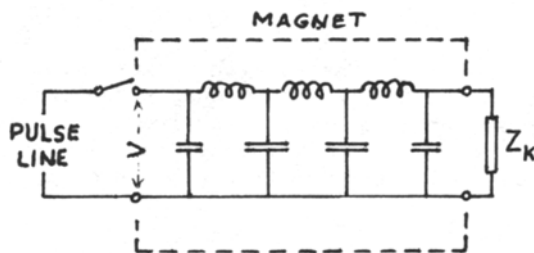
If the allowed rise time is greater than about 10 nanoseconds, a yoke of ferrite or laminated iron or met-glass may be used in either the C or H configuration (Fig. 12). To permit excitation of the magnet by a fast pulse of current, the (one-turn) winding is made of a single conductor at each side of the aperture. This then constitutes a transmission line of characteristic impedance  $Z_k = \sqrt{L'/C'}$  (Fig. 13). Equal and opposite currents flow into this line and propagate at velocity  $v_L$  to the end of the magnet where they terminate without reflection in a resistor of matched impedance. The transverse fields  $B$  and  $E$  of the line deflect the particles of the beam. One way to power such a magnet is with a storage-line pulse generator which provides a step-function voltage pulse. For such a pulsed magnet circuit, the following relations apply:

$$\begin{aligned} v_L &= 1/\sqrt{L'C'} & L' &= \mu_0 w/h \\ B &= \mu_0 I/h & V &= Z_k I = v_L w B \end{aligned} \quad (8.1)$$



XBL 868-3173

Fig. 12. Kicker magnet with capacitance indicated schematically.



XBL 868-3174

Fig. 13. Magnet shown in circuit as a lumped-element line.

A particle that traverses total length  $l$  in the magnet during the flat period of the pulse will receive an impulse

$$\Delta p_{\perp} = e l (B \pm \mathcal{E}_{\perp} / v) . \quad (8.2)$$

The upper sign applies if the pulse is traveling upstream relative to the beam, in which case the transverse electric field will aid the magnetic force. The average of  $\mathcal{E}_{\perp}$  across the aperture must be  $V/w = v_L B$ , but conductive pole tips might reduce that strength locally. The fill time of the magnet is  $l/v_L$ , but the duration  $\tau$  of the beam gap will be greater or less depending on the pulse direction according to

$$\tau = \frac{l}{v_L} \pm \frac{l}{v} . \quad (8.3)$$

For a short beam gap, large  $v_L$  would be desirable. However,  $v_L$  (and  $\tau$ ) also determine the kicker line impedance through

$$Z_K = \mu_0 \frac{w}{h} v_L = \mu_0 \frac{w}{h} / \left( \frac{1}{l} \mp \frac{1}{v} \right) . \quad (8.4)$$

In such high-power pulsed circuits, there is a practical upper limit for  $Z_K$  around 50 ohms which results in  $v_L/c \approx 0.1$  [ $w/h$  assumed  $\sim 1$  in Eq. (8.4)]. The free parameter to adjust  $Z_K$  is the distributed capacitance per unit length,  $C'$ . To add capacitance to the magnet conductor, fins are sometimes attached periodically between short sections of the kicker magnet yoke.

In seeking a set of parameters that satisfy the relations in Eq. (8.4), we note that the kicker strength does not appear in that equation. This permits one to let  $l$  represent the length of one of several separately powered short magnets. An additional argument for separate sections may come from the value of the total kicker voltage required:

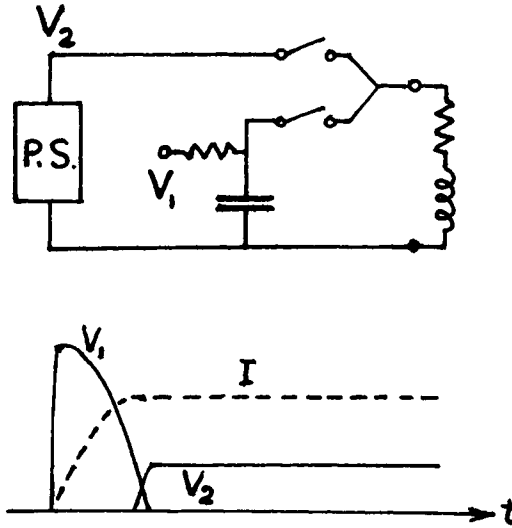
$$V = \frac{\Delta p_{\perp}}{e} \frac{w}{\tau} \frac{1 \pm v_L/v}{1 \pm \mathcal{E}_{\perp}/vB} . \quad (8.5)$$

To remain within practical limits on circuit voltage not exceeding about 100 KV, one may make several short sections, each supplied with a (suitably delayed) pulse of reasonable voltage.

In the case that the rise time is as long as the microsecond range, it is practical to make the kicker of a series of short pulsed magnets that look electrically like inductors rather than transmission lines. To produce the required rise followed by a long flat dwell, the circuit may be as in Fig. 14 to produce an initial higher voltage. This scheme is less suited to a very fast pulse because of transients between unmatched components and the more complicated voltage source.

That the kicker specifications closely define the design of the single-turn kicker appears also in the power required. During the flat portion, the power is found to be, using Eqs. (8.3), (8.4), and (8.5) in  $P = V^2/Z_K$ ,

$$P = \left(\frac{\Delta p_{\perp}}{e}\right)^2 \frac{wh (1 + v_L/v)}{\mu_0 l \tau (1 + \epsilon_{\perp}/v_B)^2} \quad (8.6)$$



XBL 868-3175

Fig. 14. Circuit and charging pulses for kicker driven as an inductor.

Finally, we point out that the single-turn magnet is a variant of the transverse stripline kicker and that the frequency-domain relations of section 4 apply, albeit with the following caveats: the symbols  $w$  and  $h$  have been interchanged,  $Z_K$  replaces  $2Z_L$ , and no transformer to  $R_0 = 50$  ohm is used. For example, from Eq. (8.6) we can find

$$\begin{aligned} R_{\perp} T^2 &= \left(\frac{\Delta p_{\perp} \beta c}{e P}\right)^2 = \mu_0 \frac{(\frac{1}{2}v)^2}{whv_L} (1 \pm \epsilon_{\perp}/v_B)^2 \\ &= Z_K \left(\frac{\frac{1}{2}v}{wv_L}\right)^2 (1 \pm \epsilon_{\perp}/v_B)^2 \end{aligned} \quad (8.7)$$

which is the same as the result of using Eq. (4.10) in the limit of small  $\theta$ .

## 9. TRANSVERSE VARIATION OF COUPLING

The problem of calculating the spatial variation of an electrode's effect across its aperture involves an integration over a three-dimensional distribution of field waves. In this section, we shall see that this can in many cases be reduced to the solution of a two-dimensional boundary-value problem.

The energy increment, expressed as a voltage  $V$ , given by a kicker to a particle passing along a straight line with constant velocity in the  $z$  direction is given, as in Eq. (1.2), by

$$V(x, y, t) = \int_a^b \vec{\mathcal{E}} \cdot d\vec{s} \quad (9.1)$$

In the integration, the value of  $\mathcal{E} = \mathcal{E}_z$  must be taken at the time  $t = z/\beta c$  when the particle passes  $z$ . For simplicity, let us omit the subscript  $z$ , then note that this  $z$ -component must satisfy the wave equation

$$\nabla^2 \mathcal{E} - \frac{1}{c^2} \frac{\partial^2 \mathcal{E}}{\partial t^2} = 0 \quad (9.2)$$

Let us now use the above to find a two-dimensional differential equation for  $V$  involving the quantity

$$\nabla_{\perp}^2 V \equiv \frac{\partial^2 V}{\partial x^2} + \frac{\partial^2 V}{\partial y^2} \quad (9.3)$$

Differentiate Eq. (9.1) and insert Eq. (9.2):

$$\nabla_{\perp}^2 V = \int_a^b (\nabla_{\perp}^2 \mathcal{E}) dz = \int_a^b \left( \frac{1}{c^2} \frac{\partial^2 \mathcal{E}}{\partial t^2} - \frac{\partial^2 \mathcal{E}}{\partial z^2} \right) dz \quad (9.4)$$

The variables  $z$  and  $t$  are related through  $z = \beta ct$ , which we use in the relation

$$\int \frac{\partial f}{\partial z} dz = f - \int \frac{\partial f}{\partial t} \frac{dt}{dz} dz + \text{const} \quad (9.5)$$

to integrate the second term of Eq. (9.4) to obtain

$$\nabla_{\perp}^2 V = - \frac{\partial \mathcal{E}}{\partial z} \Big|_a^b + \int_a^b \left( \frac{1}{c^2} \frac{\partial^2 \mathcal{E}}{\partial t^2} + \frac{1}{\beta c} \frac{\partial^2 \mathcal{E}}{\partial z \partial t} \right) dz \quad (9.6)$$

Again apply Eq. (9.5) to integrate the mixed-derivative term:

$$v_{\perp}^2 V = \left( -\frac{\partial \mathcal{E}}{\partial z} + \frac{1}{\beta c} \frac{\partial \mathcal{E}}{\partial t} \right) \Bigg|_a^b - \frac{1}{(\beta \gamma c)^2} \int_a^b \frac{\partial^2 \mathcal{E}}{\partial t^2} dz \quad (9.7)$$

Insert Eq. (9.1) and rearrange to

$$v_{\perp}^2 V + \frac{1}{(\beta \gamma c)^2} \frac{\partial^2 V}{\partial t^2} = \left( -\frac{\partial \mathcal{E}}{\partial z} + \frac{1}{\beta c} \frac{\partial \mathcal{E}}{\partial t} \right) \Bigg|_{a,t}^{b,t + \frac{b-a}{\beta c}} \quad (9.8)$$

The solution of Eq. (9.8) is the desired function. In many applications involving kickers, accelerating electrodes, and pickups, the limits  $a$  and  $b$  may be chosen where the fields are zero or alike, making the right-hand side zero; Eq. (9.8) then simplifies to the modified wave equation

$$v_{\perp}^2 V + \frac{1}{(\beta \gamma c)^2} \frac{\partial^2 V}{\partial t^2} = 0 \quad (9.8a)$$

Boundary values are determined by Eq. (9.1) using fields at the transverse perimeter of the region of interest. For example, the fields around electrodes and gaps at the edge of the aperture may be readily known or estimated.

A familiar example of this problem is that of a narrow annular accelerating gap of length  $l$  in a circular beam tube of radius  $r_0$ . Assume the voltage across the gap as a function of azimuth  $\phi$  is  $V_0(\phi)e^{j\omega t}$ . With some assumption about how  $\mathcal{E}(r_0)$  in the gap is distributed, Eq. (9.1) can be integrated to give a transit time factor. For example, if  $\mathcal{E}(r_0)$  is rather constant across the gap at each azimuth, the boundary value  $V(r_0)$ , considered a phasor, is

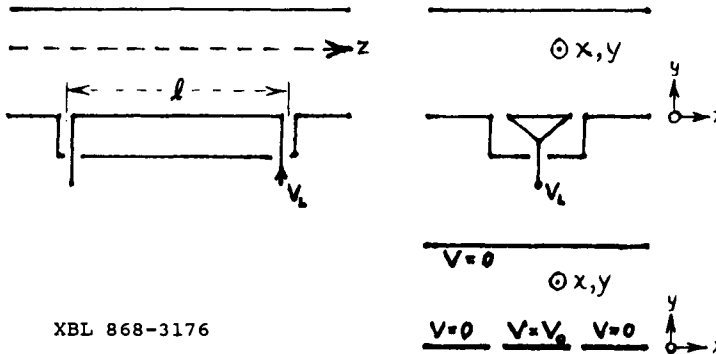
$$V(b, \phi) = \int_{-l/2}^{l/2} \mathcal{E}(r_0, \phi) e^{jk_0 z / \beta} dz \approx V_0(\phi) \frac{\sin \theta}{\theta} \quad (9.9)$$

in which  $\theta = k_0 l / 2\beta$ . If we Fourier analyse  $V_0(\phi)$ , then for each azimuthal harmonic  $V_{0n}$ , the solution of Eq. (9.8a) is found in terms of the modified Bessel functions  $I_n(k_0 r / \beta \gamma)$ . A well-known result for azimuthally uniform  $V_0$  is

$$V(r) = V_0 \frac{I_0(k_0 r / \beta \gamma)}{I_0(k_0 r_0 / \beta \gamma)} \frac{\sin \theta}{\theta} \quad (9.10)$$

One notes here that although the rf fields in an accelerating cavity may be related to  $J_n(kr)$ , that particular radial dependence does not appear in the voltage gain given to particles at various radii in the beam tube.

In the case of the stripline loop electrode, it is the application of Eq. (9.8a) that, with some restrictions, justifies the commonly employed procedure of using a 2-dimensional static electric potential distribution to calculate the spatial variation of kick  $V(x,y)$ . To illustrate this, consider the recessed loop sketched in Fig. 15. Excited by voltage  $V_L e^{j\omega t}$  fields, longitudinal electric fields in the  $y = 0$  plane appear only in the gap near



XBL 868-3176

Fig. 15. Stripline geometry and corresponding boundary-value specifications.

the ends of the stripline. If those gaps are small compared to the reduced wavelength  $\beta/k_0$ , the voltage gain seen by a particle passing along  $y = 0$  at the stripline is effectively equal to the sum of the gap voltages with appropriate phase factors. Evaluate Eq. (9.1) at the strip at  $y = 0$ :

$$\begin{aligned}
 V_0 &= \int_{-l}^0 \epsilon_2 e^{jk_0 z/\beta} dz \equiv -V_L e^{jk_0 l/\beta_L} e^{-jk_0 l/\beta} + V_L \\
 &= 2V_L e^{j(\frac{\pi}{2} - \theta)} \sin \theta \tag{9.11}
 \end{aligned}$$

where  $\theta = k_0 \frac{l}{2} (\frac{1}{\beta_L} + \frac{1}{\beta})$  as in Eq. (4.4). For any trajectory at the coordinates  $x,y$ , the particle will receive voltage  $V$  given by the solution of Eq. (9.8a) for the boundaries shown in the axial view with  $V_0$  on the strip cross section. Note that only for highly relativistic ( $\beta\gamma \gg 1$ ) particles does Eq. (9.8a) reduce to Laplace's equation for which  $V$  may be a two-dimensional electrostatic distribution. The g-factors given in Eqs. (4.2) and (4.7) are found from the ratio of  $V$  to  $V_0$  for the case of large  $\beta\gamma$ .

If the grounded wall around the strip at  $y = 0$  were moved back to make the plate a salient or protruding, the so-modified "gaps" at the ends may require the introduction of a transit-time factor and an increase in the effective length. Also, the effective width of the strip would be less simply defined. Still this method is useful

for simplifying the calculation of  $V$  and guiding the understanding of electrode geometries.

Using Eq. (9.8a) we can now understand what are the restrictions in order that the diagonally cut cylindrical difference electrode, described in section 5, will exhibit a response linear to displacement. The form of  $V$  at the boundary will contain  $\sin(\ell - L/2)k/\beta$ . With a diagonal cut,  $\ell$  varies linearly with transverse beam position. Thus, the requirements for a linear characteristic are that both  $k_0\ell$  and  $ky/\beta\gamma$  be small compared to unity.

#### REFERENCES

1. J. Borer and R. Jung, "Diagnostics," CERN/LEP-BI/84-14 (October 1984), with extensive bibliography.  
R. Littauer, "Beam Instrumentation," ed. M. Month, AIP Conf. Proc. 105, 869 (1983).
2. R. E. Colin, Foundations for Microwave Engineering, pp. 56-59, (McGraw-Hill, 1966).
3. J. Bisognano and C. Leemann, "Stochastic Cooling," eds. R. Carrigan, F. Huson, and M. Month, AIP Conf. Proc. 87, 628 (1982).
4. T. P. R. Linnecar, "The High Frequency Longitudinal and Transverse Pick-ups in the CERN SPS Accelerator," IEEE Trans. Nucl. Sci. NS-26, 3409 (June, 1979).
5. R. Shafer, "Characteristics of Directional Coupler Beam Position Monitors," IEEE Trans. Nucl. Sci. NS-32, 1933 (October, 1985).
6. D. Goldberg, G. Lambertson, F. Voelker, and L. Shalz, "Measurement of Frequency Response of LBL Stochastic Cooling Arrays for TEV-I Storage Rings," IEEE Trans. Nucl. Sci. NS-32, 2168 (October, 1985).
7. D. Boussard and G. DiMassa, "High Frequency Slow Wave Pickups," CERN-SPS/86-4(ARF), (February, 1986).
8. G. Lambertson, "The Helix as a Beam Electrode," Lawrence Berkeley Laboratory, internal report BECON-60 (August, 1985).
9. H. Yonehara, et al., INS-NUMA-49 (1983).
10. G. Lambertson, et al., "Experiments on Stochastic Cooling of 200 MeV Protons," IEEE trans. Nucl. Sci. NS-28, 2471 (June, 1981).
11. L. Faltin, "Slot-Type Pickup and Kicker for Stochastic Beam Cooling," Nucl. Instr. Methods 148, 449 (1978).
12. G. Lambertson, K. J. Kim, and F. Voelker, "The Slotted Coax as a Beam Electrode, IEEE Trans. Nucl. Sci. NS-30, 2158 (August, 1983)